Journal of Quantitative Spectroscopy & Radiative Transfer 112 (2011) 1987–1994

Contents lists available at ScienceDirect

Journal of Quantitative Spectroscopy & Radiative Transfer

journal homepage: www.elsevier.com/locate/jqsrt

Approximate analytical solution to normal emittance of semi-transparent layer of an absorbing, scattering, and refracting medium

Leonid A. Dombrovsky [a,*], Jaona H. Randrianalisoa [b,c], Wojciech Lipiński [d], Dominique Baillis [b,c]

[a] Joint Institute for High Temperatures, NCHMT, Moscow 111116, Russia
[b] CETHIL, UMR5008, CNRS, INSA-Lyon, Université Lyon 1, Villeurbanne F-69621, France
[c] LaMCoS, UMR5259, CNRS, INSA-Lyon, Université Lyon 1, Villeurbanne F-69621, France
[d] Department of Mechanical Engineering, University of Minnesota, Minneapolis, MN 55455, USA

ARTICLE INFO

Article history:
Received 4 March 2011
Received in revised form
16 April 2011
Accepted 19 April 2011
Available online 27 April 2011

Keywords:
Thermal radiation
Normal emittance
Scattering
Refraction
Analytical solution
Radiative properties

ABSTRACT

A two-step approximate analytical solution for the normal emittance of a plane layer of an absorbing, scattering and refracting medium is derived analytically. The analysis is based on the transport approximation and the two-step solution method for radiative transfer. The high accuracy of the approximate solution, examined by comparing its results to those obtained independently by the discrete ordinates and Monte Carlo methods, makes it suitable for application in combined experimental-analytical studies to identify selected spectral radiative properties of dispersed media in the range of semi-transparency.

1. Introduction

High-temperature properties of semi-transparent disperse media are pertinent to a range of engineering applications such as chemical and materials processing and energy conversion technologies. Absorption and scattering characteristics are particularly needed to analyze combined heat transfer in such media. Direct measurements of reflectance and transmittance at elevated temperatures lead to difficulties in interpreting the experimental data, associated with the presence of thermal radiation emitted by hot samples. Alternatively, normal emittance of thin isothermal samples measured at high temperatures can be used to determine temperature dependence of the absorption coefficient. While the latter approach is straightforward for non-scattering media, the identification problem becomes considerably more complex if scattering is present. An approximate analytical solution to normal emittance of a plane layer of an absorbing, scattering, and refracting medium provides a useful analytical tool for studying the effects of the problem parameters and identification of radiative properties from emittance measurements.

The objective of this paper is two-fold: (1) to present a novel approximate analytical model for the normal emittance of a refracting and scattering medium layer; and (2) to examine the accuracy of the approximate model using reference numerical solutions to the model problem. Two different numerical methods, a high-order

* Corresponding author. Tel.: +74992503264; fax: +74953625590.
E-mail addresses: dombr@online.ru, ldombr@yandex.ru (L.A. Dombrovsky).

0022-4073/$ - see front matter © 2011 Elsevier Ltd. All rights reserved.
doi:10.1016/j.jqsrt.2011.04.008

Nomenclature

A	absorptance
B	Planck function
d	sample thickness
G	incident radiation (radiation energy density)
g	function introduced by Eq. (7)
I	radiation intensity
N	number of Monte Carlo rays
n	index of refraction
R	reflectance; random number from uniform distribution (0,1)
S	radiative source function
T	transmittance
z	coordinate across the layer

Greek symbols

α	absorption coefficient
β	extinction coefficient
γ	coefficient in boundary condition (9)
ε	emittance
κ	index of absorption
μ	direction cosine
$\overline{\mu}$	asymmetry factor of scattering
ρ	reflectivity
σ	scattering coefficient
τ	optical thickness
Φ	function introduced by Eq. (14)
ω	scattering albedo

Subscripts and superscripts

a	absorbed
c	critical
e	external
i	internal
n	normal
h	hemispherical
s	scattering
t	transmitted
tr	transport
$+, -$	directions with positive and negative μ, respectively
$^{\prime\cap}$	directional-hemispherical

discrete ordinates method and the Monte Carlo method, are employed to obtain the reference solutions with maximum confidence. Furthermore, the effects of both refraction at the medium boundaries and anisotropy of volumetric scattering on the normal emittance of the medium layer are analyzed in the present study.

The traditional problem statement used in this paper may not be totally adequate to the physical reality in some cases. One should recall a contradiction between the Fresnel boundary condition and a significant volumetric scattering near the interface. This difficulty and other possible inconsistencies are discussed in the last section of the paper. Some potential applications of the suggested analytical model to identify infrared radiative properties of dispersed materials at elevated temperatures are also considered.

2. Problem statement

A plane layer of the model participating medium is shown schematically in Fig. 1. The medium is isothermal, absorbing, emitting, scattering, and refracting. The radiative properties of both the disperse phase and host medium are constant across the layer. The absorption index of the host medium is assumed to be very small as typical for semi-transparent materials in their semi-transparency ranges. The surroundings are radiatively non-participating (cold and black) and there is no external irradiation on the medium layer. As elaborated in the following sections, the effects of the following physical configurations are investigated: (i) refractive vs. non-refractive boundaries, and (ii) isotropic vs. anisotropic scattering. Note that non-refractive boundaries are encountered in a broad range of engineering problems including high-porosity fibrous insulations and foam-like materials, suspensions of particles in a gas, and other high-porosity systems.

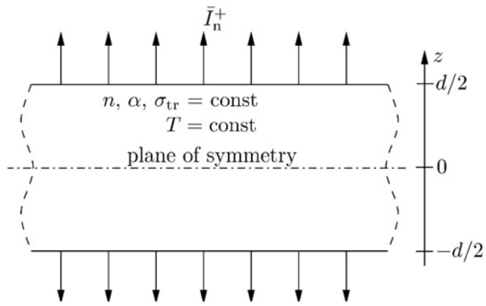

Fig. 1. Plane-parallel layer of an isothermal, absorbing, emitting, scattering, and refracting medium.

3. Approximate analytical solution for normal emittance

The two-step solution method for the radiative transfer equation (RTE) is applied to the model problem shown in Fig. 1. In this method, the transport approximation for the scattering phase function is employed in the first step. For a plane parallel isothermal layer of an absorbing, emitting, refracting, and scattering medium, the transport RTE is integrated over the azimuthal angle, leading to [1,2]

$$\mu\frac{\partial\bar{I}}{\partial\tau_{tr}}+\bar{I}=\bar{S},\quad 0<\tau_{tr}<\tau_{tr}^{0} \tag{1}$$

where $\bar{I}=I_\lambda/[2\pi n^2 B_\lambda(T)]$ is the dimensionless spectral intensity of radiation and the source function in the right-hand side of Eq. (1) is

$$\bar{S}(\tau_{tr})=\frac{\omega_{tr}}{2}\bar{G}(\tau_{tr})+(1-\omega_{tr}),\quad \bar{G}(\tau_{tr})=\int_{-1}^{1}\bar{I}(\tau_{tr},\mu)\ d\mu \tag{2}$$

Hereafter, the subscript λ is omitted for brevity. The spectral incident radiation $\bar{G}$ is proportional to the spectral radiation energy density [2]. In the above relations, $\tau_{tr}=\beta_{tr}z$ is the actual transport optical thickness, $\tau_{tr}^0=\beta_{tr}d/2$ is a half of the overall transport optical thickness of the plane layer, d is the geometrical thickness of the plane layer, $\omega_{tr}=\sigma_{tr}/\beta_{tr}$ is the transport albedo of the medium ($\beta_{tr}=\alpha+\sigma_{tr}$, $\sigma_{tr}=\sigma(1-\bar{\mu})$), and $\mu=\cos\,\theta$, where the angle θ is measured from the external normal direction. Note that Eqs. (1) and (2) are true in the case of an isotropic medium. A more complex formulation should be considered for anisotropic media when radiative properties of a small volume of the medium depend on the angle of the radiation incidence.

The boundary conditions for RTE (1) are as follows:

$$\left.\frac{\partial\bar{I}}{\partial\tau_{tr}}\right|_{\tau_{tr}=0}=0\quad \bar{I}(\tau_{tr}^0,-\mu)=\rho'^{\cap}(\mu)\bar{I}(\tau_{tr}^0,\mu),\quad \mu>0 \tag{3}$$

where $\rho'^{\cap}$ is the directional-hemispherical reflectivity of the boundary given by Fresnel's relations [2].

Normal emission is determined by finding $\bar{I}_n^+(\tau_{tr})=\bar{I}(\tau_{tr},1)$ and $\bar{I}_n^-(\tau_{tr})=\bar{I}(\tau_{tr},-1)$ from

$$\frac{d\bar{I}_n^+}{d\tau_{tr}}+\bar{I}_n^+=\bar{S},\quad -\frac{d\bar{I}_n^-}{d\tau_{tr}}+\bar{I}_n^-=\bar{S} \tag{4}$$

$$\bar{I}_n^-(0)=\bar{I}_n^+(0),\quad \bar{I}_n^-(\tau_{tr}^0)=\rho_n\bar{I}_n^+(\tau_{tr}^0),\quad \rho_n=\rho'^{\cap}(\mu=1)=\left(\frac{n-1}{n+1}\right)^2 \tag{5}$$

Note that the above expression for ρ_n is true in the case of a weakly absorbing medium with $\kappa\ll n$. The following formal solution for the normal emittance is then obtained as

$$\varepsilon_n=(1-\rho_n)\bar{I}_n^+(\tau_{tr}^0)=2\frac{1-\rho_n}{1-C_{tr}}\ \exp(-\tau_{tr}^0)\int_0^{\tau_{tr}^0}\bar{S}\ \cosh(\tau_{tr})d\tau_{tr},$$
$$C_{tr}=\rho_n\ \exp(-2\tau_{tr}^0) \tag{6}$$

An analytical relation for the source function is needed to evaluate the integral in Eq. (6). For the problem under consideration, this relation can be found using the modified two-flux approximation developed by Dombrovsky et al. [3,4]. According to this approximation, the dimensionless irradiation is expressed as

$$\bar{G}=\frac{(1-\mu_c)\bar{g}+2\mu_c(1-\omega_{tr})}{1-\omega_{tr}\mu_c},\quad \mu_c=\sqrt{1-1/n^2} \tag{7}$$

where the function $\bar{g}$ is determined by the following boundary-value problem:

$$-\frac{d^2\bar{g}}{d\tau_{tr}^2}+\zeta^2\bar{g}=2\zeta^2 \tag{8}$$

$$\bar{g}'(0)=0,\quad (1+\mu_c)\bar{g}'(\tau_{tr}^0)=-2\gamma\bar{g}(\tau_{tr}^0) \tag{9}$$

$$\zeta^2=\frac{4(1-\omega_{tr})}{(1+\mu_c)^2(1-\omega_{tr}\mu_c)},\quad \gamma=\frac{1-\rho_n}{1+\rho_n}=\frac{2n}{n^2+1} \tag{10}$$

Note that the use of normal reflectivity ρ_n in the expression for coefficient γ in Eq. (10) is an additional approximation and it may lead to a considerable error for high values of the refractive index and the scattering albedo of the medium. In a more accurate approach, one can use a value of the reflectivity averaged over the angles, $\bar{\rho}$, as it was done by Siegel and Spuckler [5]:

$$\bar{\rho}=\frac{1}{2}+\frac{(3n+1)(n-1)}{6(n+1)^2}+\frac{n^2(n^2-1)^2}{(n^2+1)^3}\ \ln\left(\frac{n-1}{n+1}\right)$$
$$-\frac{2n^3(n^2+2n-1)}{(n^2+1)(n^4-1)}+\frac{8n^4(n^4+1)}{(n^2+1)(n^4-1)^2}\ \ln\ n \tag{11}$$

The analytical solution to the above problem is as follows:

$$\bar{g}/2=1-\frac{\cosh(\zeta\tau_{tr})}{c_0+((1+\mu_c)/2\gamma)\zeta s_0},$$
$$s_0=\sinh(\zeta\tau_{tr}^0)\quad c_0=\cosh(\zeta\tau_{tr}^0) \tag{12}$$

The resulting relation for the normal emittance, derived on the basis of the modified two-flux approximation and by subsequent analytical integration of the RTE, is as follows:

$$\varepsilon_n=\frac{1-\rho_n}{1-C_{tr}}\left[1-\frac{1-\mu_c}{1-\omega_{tr}\mu_c}\frac{\omega_{tr}\Phi}{c_0+((1+\mu_c)/2\gamma)\zeta s_0}\right][1-\exp(-2\tau_{tr}^0)] \tag{13}$$

where

$$\Phi=\frac{1}{2\sinh(\tau_{tr}^0)}\left\{\frac{\sinh[(\zeta+1)\tau_{tr}^0]}{\zeta+1}+\frac{\sinh[(\zeta-1)\tau_{tr}^0]}{\zeta-1}\right\} \tag{14}$$

Obviously, these equations reduce to the well known exact formula for a non-scattering medium ($\omega_{tr}=0$) [1,2]:

$$\varepsilon_n=\frac{1-\rho_n}{1-\rho_n\exp(-\tau_a^0)}[1-\exp(-\tau_a^0)],\quad \tau_a^0=\alpha d \tag{15}$$

One can see that spectral dependences of $n(\lambda)$, $\omega_{tr}(\lambda)$, and $\tau_{tr}^0(\lambda)$ determine the spectral normal emittance of a refracting, scattering, and absorbing medium.

The derived analytical solution employs the modified two-flux approximation reported in [3,4], which enables us to determine the spectral radiation energy density. However, in the present study, this differential approximation is used only at the first stage. A subsequent integration of the RTE with the known source function at the second stage of the analytical solution makes the present approach much more accurate. A similar two-step procedure was recently analyzed by Dombrovsky and Lipiński [6] (see also [7]).

4. Numerical determination of the normal emittance

The reference numerical methods selected in this study to assess the accuracy of the approximate analytical solution employ, in contrast to the latter approach, the relation between the normal absorptance and normal-hemispherical reflectance and transmittance to indirectly determine the normal emittance of the plane layer of the uniform and isothermal medium:

$$A_n = 1 - R_{n-h} - T_{n-h} \tag{16}$$

with a subsequent use of the Kirchhoff law, $\varepsilon_n = A_n$. The normal-hemispherical reflectance, R_{n-h}, and transmittance, T_{n-h}, in Eq. (16) are computed by analyzing radiative transfer through a plane parallel cold layer exposed on one side to a normally incident collimated irradiation.

4.1. Discrete ordinate method

The discrete ordinate method (DOM) is employed as the first reference numerical method. The RTE is solved for the discrete radiative intensity field, and consequently the terms of Eq. (16) and the normal emittance are determined [1,2,8]. To mitigate the ray effect resulting from coarse angular discretization of the radiation intensity in a medium with Fresnel's boundaries, the composite DOM (CDOM) is employed [9–12]. In this method, the angular integral over the entire range of the cone angle, $-1<\mu<1$ in Eq. (2), is split into integrals over three subintervals: $-1<\mu<-\mu_c, -\mu_c<\mu<\mu_c$, and $\mu_c<\mu<1$. Subsequently, a set of quadrature points is used in each subinterval. In this study, a high order Gaussian quadrature scheme with 60 points is applied, where 20 points are used in the intervals $-1<\mu<-\mu_c$ and $\mu_c<\mu<1$, and 40 points are used in the interval $-\mu_c<\mu<\mu_c$. The details of the procedure to determine the quadrature points are given in [13]. The uncertainty in the directional-hemispherical reflectance and transmittance associated with this quadrature is estimated to be less than 5%.

4.2. Monte Carlo method

The collision-based Monte Carlo method is employed as the second reference method [13]. The terms of Eq. (16), and consequently the normal emittance, are determined statistically. A large number of stochastic rays $N_{rays} = 10^7$ is launched normally to the medium boundary $\tau_{tr} = \tau_{tr}^0$. A ray is transmitted into the medium through the upper boundary if the following relation is satisfied:

$$R_t < 1 - \rho'^{\cap} \tag{17}$$

where $\rho'^{\cap}$ is the directional-hemispherical boundary reflectivity given by Fresnel's relations for arbitrary angle of incidence. In particular, for external rays incident normally on the medium layer, $\rho'^{\cap}$ is the normal-hemispherical reflectivity, ρ_n, as defined by Eq. (5). Relation (17) is also used for internal rays incident at an arbitrary angle of incidence $\mu<\mu_c$. The location of attenuation inside the medium is determined from

$$s = -\frac{1}{\beta}\ln\ R_s \tag{18}$$

where the extinction coefficient $\beta = \alpha + \sigma$ is given by

$$\beta = \frac{2\tau_{tr}^0[1+\overline{\mu}(\omega_{tr}-1)]}{d(1-\overline{\mu})} = \frac{2\tau_a^0[1+\overline{\mu}(\omega_{tr}-1)]}{d(1-\overline{\mu})(1-\omega_{tr})} \tag{19}$$

If the following condition is satisfied

$$R_\omega < 1-\omega, \quad \omega = \frac{\omega_{tr}}{1+\overline{\mu}(\omega_{tr}-1)} \tag{20}$$

the ray is absorbed at the location of attenuation, its history is terminated, and the counter of absorbed rays N_a is updated. Otherwise, the ray is scattered and the scattering direction is determined from

$$\mu = \begin{cases} \frac{1}{2\overline{\mu}}\left[(1+\overline{\mu}^2) - \left(\frac{1-\overline{\mu}^2}{1+\overline{\mu}-2\overline{\mu}R_\mu}\right)^2\right], & \overline{\mu} \neq 0 \\ 1-2R_\mu, & \overline{\mu} = 0 \end{cases} \tag{21}$$

In Eqs. (17), (18), (20), and (21), R_t, R_s, R_ω, and R_μ are different random numbers drawn from a uniform distribution (0,1). A ray incident at the medium boundaries from within the medium and transmitted through the boundaries is considered as lost. After all N_{rays} have been traced, the normal emittance is calculated as

$$\varepsilon_n = A_n \approx \frac{N_a}{N_{rays}} \tag{22}$$

The expressions for the extinction coefficient and the scattering albedo given by Eqs. (19) and (20), respectively, have been derived using the definitions of the ordinary and transport radiative properties and the optical thickness. The explicit relations for the determination of the direction of the scattered ray (Eq. (21)) have been obtained by inverting the appropriate cumulative distribution functions [1,2]. The error of the Monte Carlo method, estimated by calculating the relative difference between the normal emittance obtained for $N_{rays} = 10^7$ and 10^6, is below 1%.

5. Results

5.1. Comparison of approximate analytical solution with reference numerical results

5.1.1. Nonrefracting medium

The boundary condition is significantly simplified in this case and the total internal reflection of the radiation at the medium boundaries is omitted from analysis. This allows for application of alternative solutions for the spectral irradiation based on the two-flux approximation or the P_1 approximation [1,2,7]. These solutions can be written in the following form:

$$\varepsilon_n = \left[1 - \frac{\omega_{tr}\Phi}{2c_0 + \zeta s_0/\gamma}\right][1-\exp(-2\tau_{tr}^0)] \tag{23}$$

The function Φ remains the same as introduced by Eq. (14), but the coefficients ζ and γ are modified as

$$\zeta^2 = (4-N_{appr})(1-\omega_{tr}) \quad \gamma = \frac{1}{2-\sqrt{1-N_{appr}N_{mod}/4}} \tag{24}$$

where $N_{appr}=0$ and $N_{appr}=1$ correspond to the two-flux and P_1 approximations, respectively. $N_{mod}=0$ and $N_{mod}=1$ correspond to Marshak's boundary condition and Pomraning's boundary condition, respectively [7]. In the limiting case of an optically thick medium, Eq. (23) is

Table 1
The normal emittance of an optically thick scattering medium.

ω_{tr}	ε_n				
	Two-flux (DP_0)	P_1	$P_{1,mod}$	DOM	MC
0.1	0.9823	0.9792	0.9804	0.9836	0.9837
0.2	0.9621	0.9558	0.9582	0.9647	0.9648
0.3	0.9389	0.9290	0.9328	0.9427	0.9428
0.4	0.9116	0.8978	0.9030	0.9166	0.9167
0.5	0.8787	0.8606	0.8674	0.8847	0.8851
0.6	0.8377	0.8150	0.8234	0.8445	0.8448
0.7	0.7842	0.7564	0.7664	0.7912	0.7914
0.8	0.7082	0.6750	0.6868	0.7147	0.7148
0.9	0.5811	0.5435	0.5563	0.5850	0.5852
0.95	0.4635	0.4263	0.4385	0.4644	0.4645

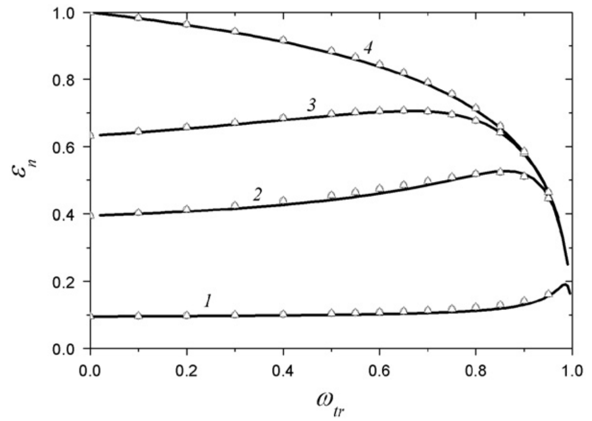

Fig. 2. Normal emittance of a layer of scattering nonrefracting medium. Comparison of the derived analytical solution (solid lines) and numerical calculations (circle points—DOM, triangle points—MC): *1*—$\tau_a^0=0.1$, *2*—$\tau_a^0=0.5$, *3*—$\tau_a^0=1$, *4*—$\tau_a^0 \gg 1$.

simplified to

$$\varepsilon_n = 1-\frac{2\omega_{tr}}{(1+\zeta)(2+\zeta/\gamma)} \tag{25}$$

A comparison of the normal emittance obtained using Eq. (25) and the reference numerical methods is presented in Table 1. Note that DOM and MC results shown in Table 1 are reported for the absorption optical thickness $\tau_a^0=10$. Additional MC computations were performed for $\tau_a^0=100$, for which the MC results remained practically unchanged with the decimal accuracy from Table 1. Good agreement is observed between the analytical and numerical results. The analytical solution based on the two-flux approximation tends to be more accurate than those based on the P_1 and $P_{1,mod}$ approximations.

A comparison of the normal emittance obtained using the analytical solution and the reference numerical methods for selected values of the absorption optical thickness $\tau_a^0=2(1-\omega_{tr})\tau_{tr}^0$ is presented in Fig. 2. One can see that the analytical results are in excellent agreement with those obtained using the reference numerical methods. Note that the presence of scattering can considerably increase the normal emittance for an optically thin medium. The latter trend was observed for the hemispherical emittance in [14,15].

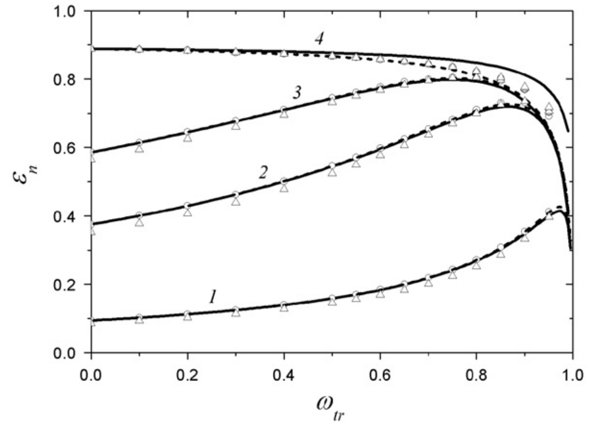

Fig. 3. Normal emittance of a layer of refracting and scattering medium at $n=2$. Comparison of the derived analytical solution (solid lines—with the use of the normal reflection coefficient in Eq. (10) and dashed lines—with the use of averaged reflection coefficient (11)) with exact numerical calculations (circle points—DOM, triangle points—MC) at $n=2$: *1*—$\tau_a^0=0.1$, *2*—$\tau_a^0=0.5$, *3*—$\tau_a^0=1$, *4*—$\tau_a^0 \gg 1$.

5.1.2. Refracting medium

A comparison of the normal emittance obtained using the analytical solution and the reference numerical methods for the refractive index of the host medium of $n=2$ is presented in Fig. 3. The agreement between the analytical solution and exact numerical results is satisfactory, and it further improves when the average reflection coefficient given by Eq. (11) is used at the first step of the analytical solution.

It is important that the effect of scattering on normal emittance is similar to that observed for the above analyzed case of $n=1$. The increase of emittance due to scattering was observed experimentally by Rozenbaum et al. [16] for optically thin samples of semi-transparent scattering materials. An equivalent result was recently obtained for absorptance of porous ceramics by Dombrovsky et al. [17]. It was noted that a porous sample of a weakly absorbing substance exhibits significant absorption in the case when numerous pores lead to very long path of photons in the sample. One should recall that according to [17] this effect can be used to determine a very low absorption coefficient of dense materials.

5.2. Effect of scattering phase function on normal emittance

In the above analysis, we considered the transport RTE assuming that it is sufficient to obtain satisfactory results for arbitrary scattering phase function of the medium. The error of the transport approximation for the problem under consideration could not be estimated by referring to the past work by the authors. Thus, additional computations are performed for anisotropic scattering phase functions to estimate this error.

The effect of the scattering phase function on the normal emittance is examined in Figs. 4 and 5. The approximate analytical solution and the reference methods give practically the same results. However, the error of DOM becomes more pronounced for the non-refracting optically thick medium ($n=1$, $\tau_a^0 \gg 10$) and high transport

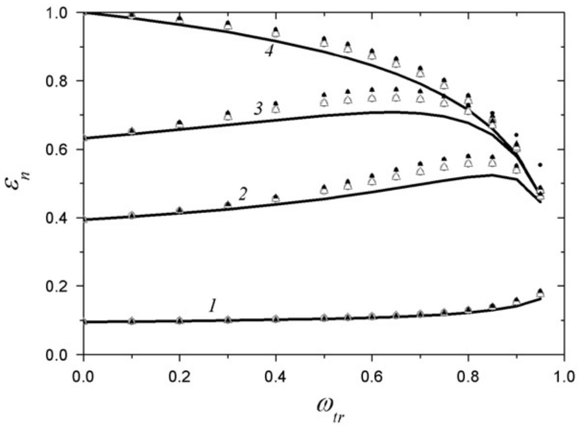

Fig. 4. Effect of scattering phase function on normal emittance of scattering nonrefracting medium. Comparison of transport approximation (solid lines) and Henyey–Greenstein approximation (circle points—DOM, triangle points—MC; big open symbols—$\overline{\mu}=0.5$, small filled symbols—$\overline{\mu}=0.9$): 1—$\tau_a^0=0.1$, 2—$\tau_a^0=0.5$, 3—$\tau_a^0=1$, 4—$\tau_a^0 \geqslant 1$.

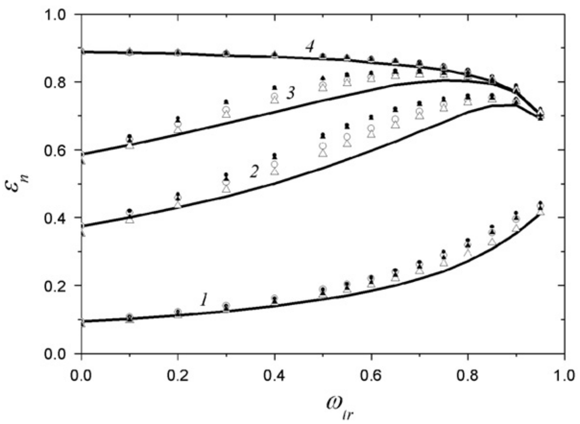

Fig. 5. Effect of scattering phase function on normal emittance of refracting and scattering medium at $n=2$. Comparison of transport approximation (solid lines) and Henyey–Greenstein approximation (circle points—DOM, triangle points—MC; big open symbols—$\overline{\mu}=0.5$, small filled symbols—$\overline{\mu}=0.9$): 1—$\tau_a^0=0.1$, 2—$\tau_a^0=0.5$, 3—$\tau_a^0=1$, 4—$\tau_a^0 \geqslant 1$.

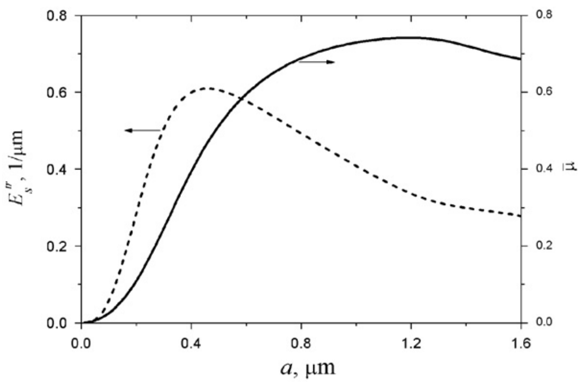

Fig. 6. Characteristics of scattering by a porous material containing monodisperse pores with radius a.

scattering albedo ($\omega_{tr}>0.8$). The scattering phase function has only a minor effect on the normal emittance. At the same time, the results obtained by the transport approximation considerably differ from the numerical ones for $\overline{\mu} \geq 0.5$, particularly for larger values of ω_{tr} and refracting samples of moderate optical thickness. Thus, typical ranges of $\overline{\mu}$ are evaluated here for selected types of scattering media. Consider the effect of pore size on the value of $\overline{\mu}$ and specific transport scattering coefficient (per unit volume fraction of pores) $E_s^{tr}=0.75Q_s^{tr}/a$ for a weakly absorbing porous material with index of refraction $n=2$ at wavelength $\lambda=3$ μm. The results of calculations using the Mie theory are presented in Fig. 6. The region of high scattering is characterized by asymmetry factor of $\overline{\mu}=0.3-0.6$. At the same time, the value of $\overline{\mu}$ is very small for pores with radius $a<0.3$ μm. Thus, $\overline{\mu}=0.5$, used in our calculations, is close to the upper estimate for strongly scattering materials, whereas $\overline{\mu}=0.9$ is typical for more specific cases.

The role of the transport approximation in the analytical approach is examined by comparing the results of the reference numerical methods employing the selected Henyey–Greenstein functions (Figs. 4 and 5) and the analytical solution using the transport approximation (Figs. 2 and 3). The transport approximation is confirmed as a suitable approach in the derivation of the approximate analytical solution. Furthermore, the validity of the transport approximation is important for identification of selected radiative properties of semi-transparent scattering materials based on the measurements of the normal emittance because it allows for the reduction of required problem parameters to the index of refraction, the absorption coefficient, and the transport scattering coefficient. As to the effect of unknown scattering phase function, it can be estimated using our computational results for different Henyey–Greenstein functions.

6. Applicability of the analytical solution

The traditional problem statement used in this paper has several physical limitations that may render it inadequate for some problems. We have already emphasized that the above analysis based on the RTE is applicable only in the case of a semi-transparent medium, which excludes the application of the approximate analytical solution for highly absorbing and almost opaque materials, i.e. in spectral ranges where thermal radiation is emitted by a very thin surface layer of thickness comparable with the wavelength. For such materials, emittance reduces to emissivity and the volumetric analysis based on the RTE becomes inadequate. The volumetric model described in this paper can, however, still be considered to model a rough surface of an opaque material by representing the structures of the rough surface by an equivalent cloud of single randomly positioned particles placed over a smooth surface of the same opaque material. The main physical features of the radiation absorption, scattering, and emission in such a cloud are expected to be similar to that by a rough surface. One should recall that a model of this type was successfully used by Dombrovsky [18] to explain the experimental data for thermal radiation of a foam on sea surface as applied to the microwave remote sensing [7].

The second type of problems for which the proposed model may be inadequate involves volumetric scattering of infrared radiation by a sample of disperse medium with an average distance between the particles (or pores) and the sample boundary comparable with the particle size and/or radiation wavelength. In this case, the total internal reflection is practically not observed, contrasting to the assumption of Fresnel's boundaries in the present model. The true index of refraction of the host medium should then be replaced by an effective index of refraction of the heterogeneous medium.

The above discussion leads to the conclusion that the choice of an appropriate physical model cannot be formalized. This difficulty is a direct consequence of the phenomenological character of the traditional radiation transfer theory. At the same time, a rigorous analysis based on the electromagnetic wave theory is usually computationally too demanding to be applied to real engineering systems.

Examples of previous pertinent studies on high-temperature emittance characterization of semi-transparent media can be found in [19–24]. The main challenge of the experimental procedure is related to isothermal heating of a sample by uniform external irradiation, e.g. using lasers or arc-lamps [20,23,24]. In the works of Rozenbaum et al. [19], Manara et al. [22], and Delmas et al. [23], the emittance was obtained by employing both experimental and theoretical methods. The theoretical methods were complex such as ray tracing or DOM. As a result, the formal inverse problem solution may be time consuming. Lopes et al. [21] identified radiative properties of opaque packed spheres from inverse method combining radiation measurements and theoretical modeling. Theoretical directional spectral emittance of an absorbing and scattering isothermal system of packed spheres is predicted by a radiative model based on the discrete ordinates method.

Thus, it is more practical to use simpler modeling techniques such as the current approximate analytical solution. Indeed, to determine the infrared radiative properties of a dispersed material at elevated temperatures, one can combine the results of ordinary measurements at room temperature and the normal emittance measurements at a high temperature. This method was used in the recent study [24]. It was assumed that the sample porosity, the index of refraction, and the transport scattering coefficient are practically independent of temperature. This assumption is supported by the known experimental data [25] and it is expected to be correct in the range of semi-transparency, at least far from the Christiansen wavelength, where $n=1$. In this combined approach, a variation of the normal emittance with temperature is treated as a result of a temperature variation of the absorption coefficient.

The analytical solution for normal emittance allows for verification of the identification procedure of the absorption coefficient based on the emittance measurements. Such verification is needed because inverse radiative transfer problems are typically ill-posed. Consider the

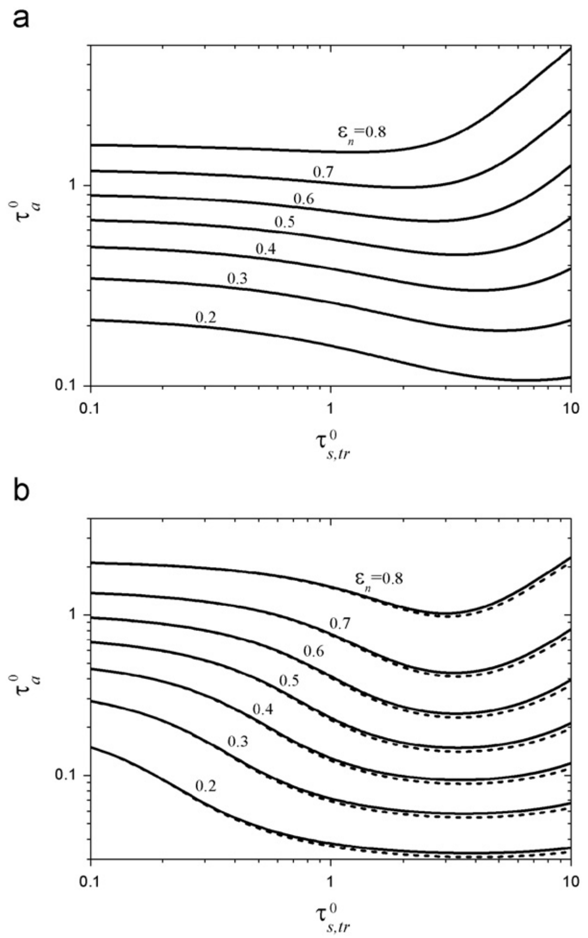

Fig. 7. Isolines of the normal emittance in the plane of $(\tau_{s,tr}^0, \tau_a^0)$ for (a) $n=1$ and (b) $n=2$. Solid lines are obtained with the use of the normal reflection coefficient in Eq. (10) and dashed lines—with the use of averaged reflection coefficient (11).

lines of constant normal emittance in a plane of $(\tau_{s,tr}^0, \tau_a^0)$, where $\tau_{s,tr}^0 = \sigma_{s,tr} d = \tau_a^0 \omega_{tr}/(1-\omega_{tr})$. One can see in Fig. 7 that the value of τ_a^0 can be determined from the measurements of ε_n for known values of $\tau_{s,tr}^0$. This important result confirms that the procedure employed by Dombrovsky et al. [24] to determine high-temperature absorption coefficient of a porous zirconia ceramics is correct. Note that another problem statement does not provide a unique result: one can find two different solutions for the transport scattering coefficient for known normal emittance and absorption coefficient of the medium. It is clear from Fig. 7 that relatively small scattering has no effect on the identification of the absorption coefficient, but the effect of scattering increases considerably in the case of a refracting host medium.

7. Conclusions

A two-step approximate analytical solution to the normal emittance of a plane parallel layer of an absorbing, emitting, scattering, and refracting medium is derived analytically. The derivation is based on the transport approximation and the two-step solution method for radiative transport.

The accuracy of both the transport approximation and the two-step approximate analytical solution is examined by comparing its results to those obtained using reference discrete ordinates and Monte Carlo methods. The accuracy of the two-step approximate analytical solution is satisfactory in all cases investigated, making the approximate solution suitable for practical applications such as identification of radiative properties, in particular the absorption coefficient of scattering materials such as porous ceramics, based on measurements of normal emittance. In the latter case, the scattering properties should be obtained independently.

The traditional problem statement used in this paper may be inadequate to the physical reality in some cases. One should recall a contradiction between the Fresnel boundary condition and a significant volumetric scattering near the interface as well as thermal radiation in opacity spectral ranges when very thin samples appear to be optically thick and surface effects are predominant. In the latter case, one can consider a similar approach to model the effect of surface roughness assuming the independent absorption and scattering by the surface elements.

Acknowledgements

The first author is grateful to the Russian Foundation for Basic Research (Grant 10-08-00218a) for the financial support of this study.

References

[1] Siegel R, Howell JR. Thermal radiation heat transfer. 4th ed. New York: Taylor & Francis; 2002.
[2] Modest MF. Radiative heat transfer. 2nd ed. New York: Academic Press; 2003.
[3] Dombrovsky L, Randrianalisoa J, Baillis D, Pilon L. Use of Mie theory to analyze experimental data to identify infrared properties of fused quartz containing bubbles. Appl Opt 2005;33:7021–31.
[4] Dombrovsky L, Randrianalisoa J, Baillis D. Modified two-flux approximation for identification of radiative properties of absorbing and scattering media from directional-hemispherical measurements. J Opt Soc Am A 2006;23:91–8.
[5] Siegel R, Spuckler CM. Approximate solution methods for spectral radiative transfer in high refractive index layers. Int J Heat Mass Transfer 1994;37(Suppl. 1):403–13.
[6] Dombrovsky L, Lipiński W. A combined P_1 and Monte Carlo model for multi-dimensional radiative transfer problems in scattering media. Comput Thermal Sci 2010;2:549–60.
[7] Dombrovsky LA, Baillis D. Thermal radiation in disperse systems: an engineering approach. New York and Redding (CT): Begell House; 2010.
[8] Coelho PJ. Bounded skew high order resolution schemes for the discrete ordinates method. J Comput Phys 2002;175:412–37.
[9] Liou B-T, Wu C-Y. Radiative transfer in a multi-layer medium with Fresnel interfaces. Heat Mass Transfer 1996;32:103–7.
[10] Wu C-Y, Liou B-T. Discrete-ordinate solutions for radiative transfer in a cylindrical enclosure with Fresnel boundaries. Int J Heat Mass Transfer 1997;40:2467–75.
[11] Muresan C, Vaillon R, Menezo C, Morlot R. Discrete ordinates solution of coupled conductive radiative heat transfer in a two-layer slab with Fresnel interfaces subject to diffuse and obliquely collimated irradiation. J Quant Spectrsc Radiat Transfer 2004;84: 551–62.
[12] Randrianalisoa J, Baillis D, Pilon L. Improved inverse method for radiative characteristics of closed-cell absorbing porous media. J. Thermophys. Heat Transfer 2006;20:871–83.
[13] Farmer JT, Howell JR. Comparison of Monte Carlo strategies for radiative transfer in participating media. Adv Heat Transfer 1998;31:333–429.
[14] Dombrovsky LA. Calculation of radiation heat transfer in a plane-parallel layer of absorbing and scattering medium. Fluid Dynamics 1972;7:691–5.
[15] Dombrovsky LA. Radiation heat transfer in disperse systems. New York: Begell House; 1996.
[16] Rozenbaum O, De Sousa Meneses D, Echegut P. Texture and porosity effects on the thermal radiative behavior of alumina ceramics. Int J Thermophys 2009;30:580–90.
[17] Dombrovsky LA, Tagne HK, Baillis D, Gremillard L. Near-infrared radiative properties of porous zirconia ceramics. Infrared Phys Tech 2007;51:44–53.
[18] Dombrovsky LA. Calculation of the thermal radiation emission of foam on the sea surface. Izvestiya—Atmos Ocean Phys 1979;15: 193–8.
[19] Rozenbaum O, De Sousa Meneses D, Auger Y, Chermanne S, Echegut P. A spectroscopic method to measure the spectral emissivity of semi-transparent materials up to high temperature. Rev Sci Instrum 1999;70:4020–5.
[20] Lopes R, Delmas A, Sacadura J-F. A new experimental device to measure directional spectral emittance of semitransparent media at high temperatures. High Temp–High Press 2000;32:369–76.
[21] Lopes R, Moura LM, Baillis D, Sacadura J-F. Directional spectral emittance of a packed bed: correlation between theoretical prediction and experimental data. ASME J Heat Transfer 2001;123:240–8.
[22] Manara J, Reidinger M, Korder S, Arduini-Schuster M, Fricke J. Development and characterization of low-emitting ceramics. Int J Thermophys 2007;28:1628–45.
[23] Delmas A, Robin-Carillon L, Oelhoffen F, Lanternier T. Experimental and theoretical characterization of emission from ceramics at high temperature: investigation on yttria-stabilized zirconia and alumina. Int J Thermophys 2010;31:1092–110.
[24] Dombrovsky LA, Rousseau B, Echegut P, Randrianalisoa JH, and Baillis D. High temperature infrared properties of YSZ electrolyte ceramics for SOFCs: experimental determination and theoretical modeling. J Am Ceramic Soc, in press.
[25] Eldridge JI, Spuckler CM, Markham JR. Determination of scattering and absorption coefficients for plasma-sprayed yttria-stabilized zirconia thermal barrier coatings at elevated temperatures. J Am Ceramic Soc 2009;92:2276–85.